Upgrade and Modification of a Machine for Micro-Abrasion Wear Testing in Simulated Biological Environments with Oscillatory Motion

Actualización y modificación de una máquina para ensayos de micro abrasión-desgaste en entornos biológicos simulados con movimientos oscilatorios

Diego F. Prieto[1], José L. Caballero[2], Willian A. Aperador[3] and Juan H. Martínez[4]

ABSTRACT

Aiming to evaluate the useful life of biomaterials used in joint prostheses, this study performed different wear tests in stainless steel 316L, a biomaterial used in hip joint replacements. The tests were carried out in a dry medium, with the help of an equipment that was improved regarding some of its characteristics and allows conducting wear tests via the contact of two bodies, one of them being the biomaterial under study and the other one a sphere of a harder material. For the evaluation, a device was developed to change the rotation of the sphere, varying the angle it traveled and the frequency with which it did it. Once the improvements were made to the aforementioned equipment, tests were conducted which involved obtaining wear tracks in order to observe the surface morphology through scanning electron microscopy (SEM) and to measure the length and the width of the tracks, with which the biomaterial wear coefficient was obtained for each case studied. In these tests, the wear coefficient showed variations with respect to the sphere's angle of travel.

Keywords: wear, biomaterial, scanning electron microscopy, reciprocating motion

RESUMEN

Con el objetivo de evaluar la vida útil de los biomateriales utilizados en prótesis articulares, este estudio llevó a cabo ensayos de desgaste en acero inoxidable 316L, un biomaterial usado en prótesis articulares de cadera. Los ensayos se realizaron en seco, con la ayuda de un equipo que se mejoró en algunas características y que permite realizar ensayos de desgaste mediante el contacto de dos cuerpos, siendo uno de estos el biomaterial a estudiar y el otro una esfera de un material más duro. Para la evaluación se desarrolló un dispositivo para cambiar el giro de la esfera, variando el ángulo que recorría y la frecuencia con la que lo hace. Una vez realizadas las mejoras al equipo mencionado, se realizaron ensayos donde se obtuvieron huellas de desgaste para observar la morfología superficial mediante microscopía electrónica de barrido (SEM) y medir el largo y el ancho de las huellas, con los cuales se obtuvo el coeficiente de desgaste del biomaterial para cada caso estudiado. En estas pruebas, el coeficiente de desgaste presentó variaciones con respecto al ángulo de recorrido de la esfera.

Palabras clave: desgaste, biomaterial, microscopía electrónica de barrido, movimiento reciprocante

Introduction

Since ancient times, humans have sought to improve their quality of life, a field that has been widely developed thanks to many advances. This, in addition, has made it possible to increase people's life expectancy, allowing them to live long and healthy lives, which represents a challenge for field of healthcare, given that, as one becomes older, diseases tend to emerge which are complex to treat (Gómez and Sabeh, n.d.).

The United Nations Population fund (UNFPA) submitted a report detailing that, by 2050, one in five people will be over 60 old, which also means that there will be more people over 60 than under 15 years old. In addition, it is expected

[1] Mechatronics engineer, Universidad Militar Nueva Granada, Colombia. Master in Mechatronics Engineering, Universidad Militar Nueva Granada, Colombia. Affiliation: Consultant, Management Solutions, Colombia. Email: diegofelipe-prietomorales@gmail.com

[2] Mechatronics engineer, Universidad Militar Nueva Granada, Colombia. Master in Mechatronics Engineering, Universidad Militar Nueva Granada, Colombia. Affiliation: Professor, Universidad Militar Nueva Granada, Colombia. Email: jose.caballero@unimilitar.edu.co

[3] Physicist, Universidad Pedagógica y Tecnológica de Colombia, Colombia. PhD in Engineering, Universidad del Valle, Colombia. Affiliation: Professor, Universidad Militar Nueva Granada, Colombia. Email: william.aperador@unimilitar.edu.co

[4] Mechanical engineer, Universidad Central, Colombia. Master in Mechanical Processes, Universidad Nacional de Colombia. Affiliation: Professor, Universidad Militar Nueva Granada, Colombia. Email: juan.martinezp@unimilitar.edu.co

that the number of inhabitants who are around 80 years of age will multiply by five. Massive longevity has individual implications related to maintaining the quality of life, as well as new social and economic challenges that, if left unsolved, will cause people to lack the optimal conditions for living (BBC, 2012).

These sociological factors have driven a breakthrough in biomaterials, as well as research in this field. Furthermore, technological and medical advances allowed improving surgical techniques, which resulted in a greater use of prostheses, implants, medical systems, and devices that must usually be in contact with body tissues (BBC, n.d., 2012).

Biomaterials must have certain characteristics in order for them to be used in patients. One of the most critical is the compatibility of a biomaterial with the patient and the assurance of a long half-life, a factor that is currently being increased, given that, by prolonging the useful life of the biomaterial, future interventions on the patient are avoided, which are inherently risky (Vallet, 2004).

In light of the above, some factors involved in the extension of the useful life of a biomaterial when in external or internal contact with the body have been highlighted by the literature, *i.e.*, the reduction of friction between the interacting materials – where wear must be minimized – and the implementation of methods to prevent and control the corrosion of materials, such as the deposition of coatings and a correct selection of materials (Caicedo *et al.*, 2013; Rasor, 2009).

Several tests are being carried out to find new biomaterials capable of efficiently withstanding the wear produced by the body's internal fluids and by the friction of the body itself. One of these is micro-abrasion wear testing, which has different variations and involves several systems, aiming to determine the characteristics of the analyzed material.

The purpose of this paper is to present an improvement plan for micro-abrasion wear testing equipment. Different mechanisms were built, adapted, and coupled with the system, and an invertible turning mechanism was incorporated, seeking to recreate typical movement behaviors in joint replacements, specifically the hip.

Calculating micro-abrasive wear

Tribology is a science that studies the friction, wear, and lubrication phenomena of surfaces with relative motion. It is a science that interrelates different fields of study such as chemistry, physics, and mechanics, among others (Losada-Prieto *et al.*, 2001). Tribological tests employ different standards according to the type of test to be performed and the mechanism used to carry it out.

This research analyzes the results obtained from a system used for micro-abrasion tests (Figure 1), with a variant called *fixed-ball*.
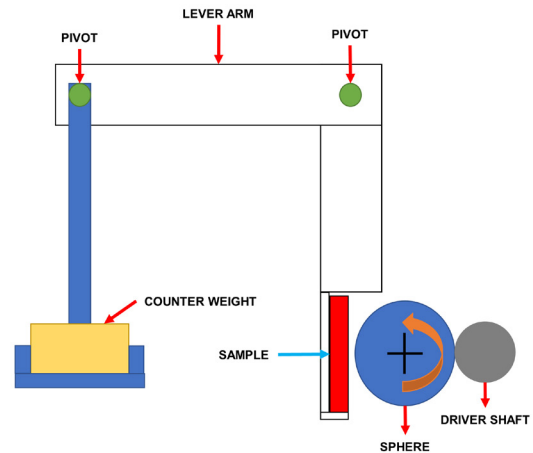
Figure 1. Schematic diagram of the fixed-ball test
Source: Authors

In this test, the sphere rotates in just one direction, and it is clamped against two coaxial transmission shafts that allow it to be easily removed and replaced. The square specimen is pressed by the rotating sphere from the side by means of loads placed on the test stand (Gant and Gee, 2011). The contact between the sphere and the specimen creates friction, which subsequently generates a crater-shaped wear track (Staia *et al.*, 1998).

Normally, micro-abrasion tests, as the name suggests, are carried out with an abrasive fluid, but this type of system can also be used to carry out lubricated or dry sliding tests.

Conventional systems have a limitation when it comes to testing, since the sphere rotating with the sample cannot perform reversals. Thus, its operation clearly involves only one direction at a certain speed. The equipment developed in this research, however, can perform tests with rotation inversion and a certain angle of travel at a desired frequency.

This article presents different mathematical models that allow relating the dimensions of the tracks obtained during testing with a rate of volume loss and a constant wear rate. Therefore, after each test performed, parallel and perpendicular measurements of each track were taken (Figure 2), and an average of these measurements was calculated, since, for each study case, two tests were performed in order to obtain reliable diameter values.

To analyze the measurements of wear tests, some authors state that the wear volume of the sample is given by the following equation, taking into account that $b \ll R$ (Gee *et al.*, 2002; Sampaio *et al.*, 2016; Caballero *et al.*, 2016):

$$V = \pi \frac{b^2}{64R} \qquad (1)$$

where R is the radius of the sphere and b is the diameter of the crater generated during the test. Once the wear volume
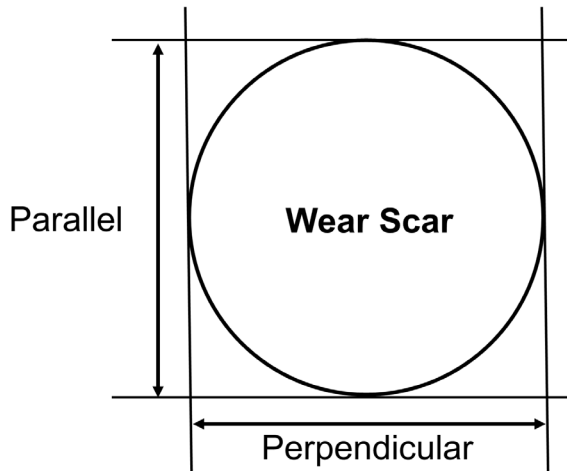
Figure 2. Measurement of wear track
Source: Authors

has been determined, the Archard relation is used, which relates the wear volume to the normal load N and the sliding distance S:

$$V = K_c SN \qquad (2)$$

Equating (1) and (2) describes the wear coefficient as:

$$K = \frac{\pi b^4}{64R} \frac{1}{SN} \qquad (3)$$

To calculate the sliding distance S for a continuous rotation of the system, the following relation is used:

$$S \quad \# cycles * 2 * \pi * R \qquad (4)$$

When tests are performed with reciprocating rotation, with an angle of travel β expressed in degrees, the sliding distance S is determined as follows:

$$S = \frac{\# cycles * \beta * 4 * \pi * R}{360} \qquad (5)$$

Materials and methods

To develop the improvement plan, some aspects were taken from the roadmap for engineering design (Figure 3), which considers different elements that allow carrying out each proposed task.
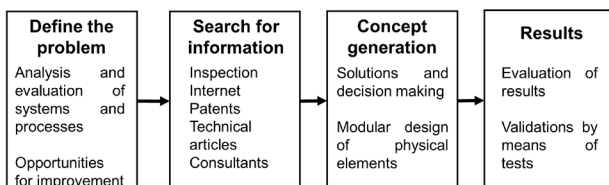

Figure 3. Modified engineering design roadmap
Source: Authors

The redesign sought to improve the existing system. In this process, there can be different tasks aimed to improve the operation of certain components, thus allowing the general assembly to work properly. It is worth noting that the redesign is achieved without any change in the operating principle or the original concept of the evaluated system (Dieter and Schmidt, 2009).

For the project, some parts assemblies were redesigned, and one system was replaced, which improved the functionality of the equipment.

There is no single formula for a viable design or redesign; several authors have different methods, although one of the simplest and most accepted, which is taken as a basis for other models, is the one given by Morris Asimow, who believed that a process can be framed in different cyclical design operations resulting in a product (Dieter and Schmidt, 2009).
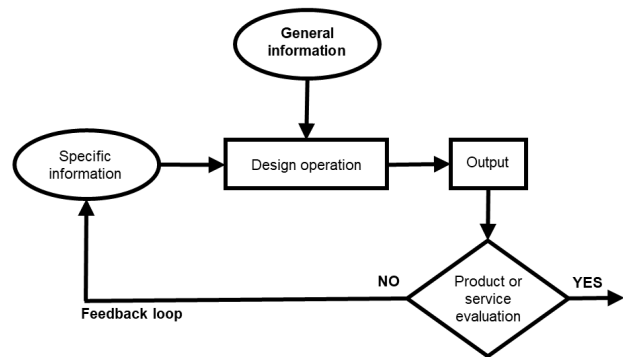
Figure 4. Basic module of the design process
Source: Authors

Based on Figure 4, it can be inferred that design is a sequential process consisting of multiple design operations, where one moves to the next step after evaluating whether what has been done satisfies the required specifications.

Design can be approached as a problem to be solved. The methodology selected for solving the problems involved in the improvement plan designed in this research consist of the following steps (Dieter and Schmidt, 2009):

- Defining the problem
- Collecting information
- Generating solutions and decision-making
- Results (testing)

Experimentation

Defining the problem

To develop the improvement plan, the starting point was a system (Figure 5) for conducting wear and micro-abrasion tests which has a square profile structure with a lever arm,

where there are counterweights that, when moved along the axis that supports them, apply a certain load to the sample under analysis. A dynamometer is used to determine the load exerted by the dead weight and the counterweight. Moreover, there is a sphere that rotates against the sample for a certain number of cycles and at certain velocity, producing wear and abrasion on the sample.
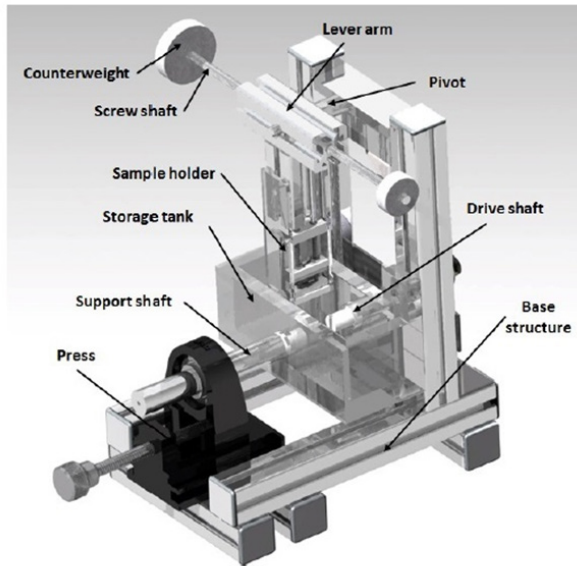
Figure 5. Micro-abrasion testing equipment
Source: Caballero *et al.* (2016)

Based on an analysis of the system's operation, the most important requirements for any user are the compatibility of the samples, the modularity of the system, and the accuracy of the tests. These factors are fundamental in equipment for materials testing, which is why the possible points for improvement are framed in the requirements mentioned Table 1 (Caballero *et al.*, 2016).

In addition, it was observed that, in most studies involving fixed-ball micro-abrasion tests, multiple parameters are varied, such as, the sample and sphere material, the applied loads, whether the test is performed dry or with abrasive particles, among others, without considering that the movement of the sphere could be oscillatory and have a certain angle of travel, which, depending on the application, could be modified at will (Stachowiak *et al.*, 2006; Cozza *et al.*, 2009; Ardila *et al.*, 2020).

The materials to be used in a biological environment, specifically inside the human body (*e.g.*, prostheses), can have oscillatory movements, as is the case of hip replacements, which participate in human motion (Figure 6).

Due to the above, this study proposes that the most significant change to the system will be allowing to invert the rotation of the sphere in contact with the analyzed sample. It is stressed that the system will be able to vary the rotation of the sphere to any desired value.

Collecting information

An inspection of the equipment revealed four points for improvement and the possibility of changing one of its systems, with the aim to improve the equipment's performance.
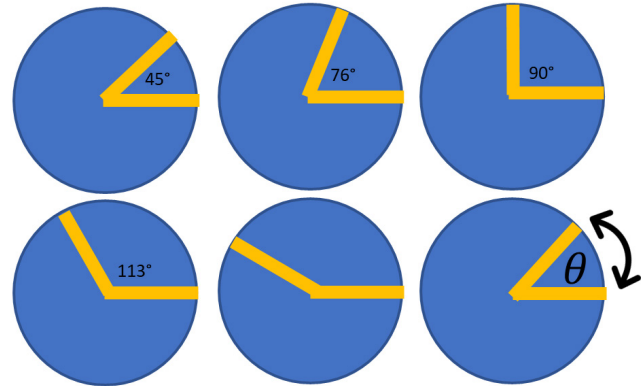
Figure 6. Turning angles of the hip during human motion
Source: Authors
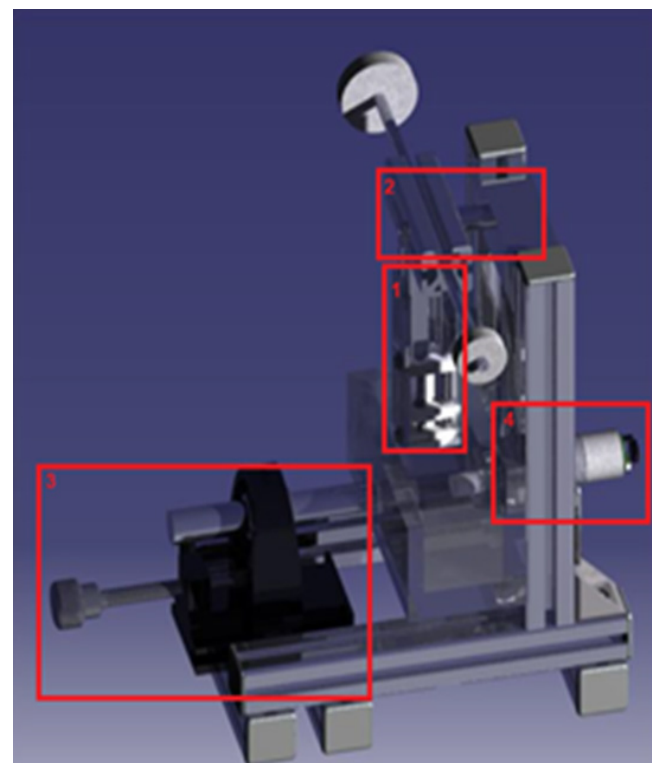
Figure 7. Current micro-abrasion testing system: 1) specimen clamping, 2) arm clamping, 3) sphere clamping, 4) motor system
Source: Adapted from Caballero *et al.* (2016)

The above-presented elements and assemblies (Figure 7) were subjected to different modifications, which allowed for some variations in the tests performed.

Below is a table with the improvement points, the characteristics to be improved, and the proposed solutions.

Table 1. Improvement points for the micro-abrasion testing system

| Subsystem	Feature to improve	Solution implemented
Specimen clamping	Although the system has an outstanding grip, it limits the shape of the samples that can be analyzed. Additionally, in some tests, it was observed that the sample showed a slight movement, which could generate variations in the test results.	A circular cut was made in the parts that exert pressure on the sample, which is now a circular sample holder, which will allow the clamping to be more stable. A cut was made on the lateral plates, which avoids their contact with the sphere clamping system, thus avoiding misalignments.
Sample connector arm	The assembly is stable and allows the support to hold the specimen at the end of the square profile that composes it, although it only allows for one degree of freedom (vertical), since the bearing is housed inside the support and does not allow the pivot to move horizontally.	The element that holds the shaft connecting the sample arm to the support was replaced by a bearing, allowing for an additional degree of freedom (horizontal).
Sphere clamping	This subsystem consists of a support shaft on which the sphere rests. The support shaft rests on a bearing that is positioned at the top of the press. The limitation of the clamping system is that the press is oversized for the function that it must perform, and it takes up a large amount of space in the assembly of the system. Additionally, there is no certainty as to how much force the press exerts on the sphere and therefore on the motor shaft (this is adjusted manually).	To hold the sphere, a system with a plunger was designed, which will be responsible for exerting a certain pressure on the sphere, so that it is not offset during the tests.
Motor, drive shaft, and bushing	The current system has a DC motor, which has a magnetic encoder coupled to its shaft. This motor is controlled by a DAQ data acquisition card. The motor used in the current system, together with its respective encoder, are difficult to manipulate, since they require an acquisition system that can process the pulses of the encoder, which, being magnetic, have high frequencies and do not feature rotation inversion.	The DC motor was replaced by a stepper motor (Nema 17), which does not require a sensor, since each of its steps reports exactly how many degrees the motor shaft moves. A bushing was designed to allow for a solid coupling between the motor and the drive shafts. The drive shaft was designed with a smaller diameter in the part where it comes into contact with the groove of the sphere, preventing it from colliding with the sample.

Source: Authors

Generating solutions and decision-making

Based on Table 1, the following images show the development of the improved subsystems.
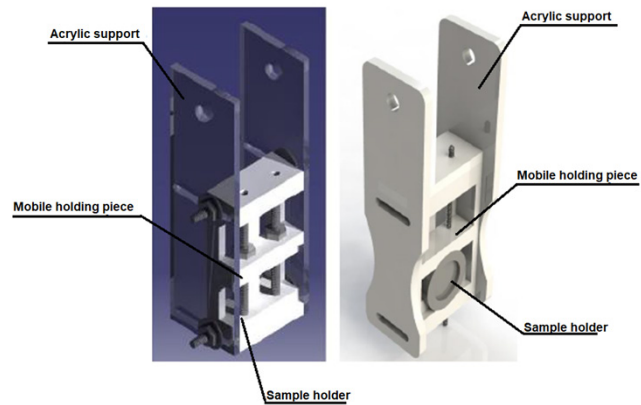
Figure 8. Fastening system: a) current b) redesigned
Source: Authors

Figure 8 shows that the sample holder and the mobile holding part were made with EMPAC. In the redesign, they were manufactured by means of 3D printing.
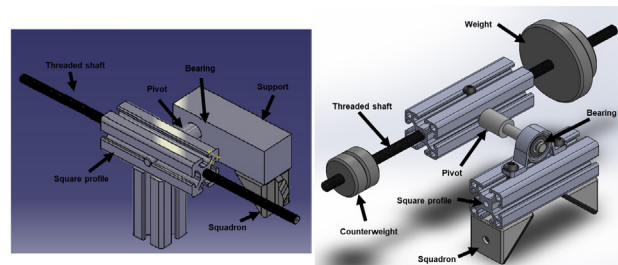
Figure 9. Sample connector arm clamping system: a) current b) redesigned
Source: Authors

Figure 9 shows how the rigid support that contained the bearing that in turn supported the pivot connected to the counterweight system was replaced by a square profile tube on which a bearing rests, thus allowing the system to move horizontally as needed.
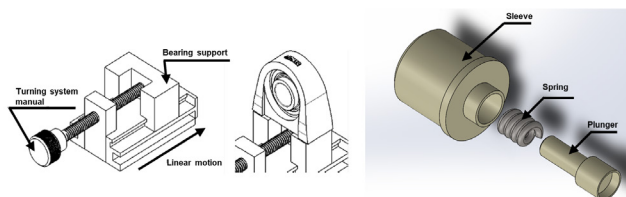
Figure 10. Sphere clamping system: a) current b) redesigned
Source: Authors

For the calculation of the spring (Figure 10), it is necessary to keep the sphere pressed against the shaft that connects to the motor. To find the spring constant to be used, the force exerted vertically by the sphere must first be calculated.

$$\textit{Sphere mass} = 0{,}11074 \; \textbf{\textit{kilograms}}$$

$$\mathbf{F = m * g} \tag{6}$$

$$\mathbf{F = 0{,}11074\,Kg * 9{,}8\,\dfrac{m}{S^2}} \tag{7}$$

$$\mathbf{F = 1{,}086\,Newton} \tag{8}$$

Considering a 10% safety factor, the vertical force exerted by the sphere is:

$$\mathbf{F_{sphere} = 1{,}10 * F} \tag{9}$$

$$\mathbf{F_{sphere} = 1{,}10 * 1{,}086\,N} \tag{10}$$

$$\mathbf{F_{sphere} = 1{,}19\,Newton} \tag{11}$$

The spring recoil is approximately 14 mm, which is equal to the Δx that the spring must have when it compresses the sphere. From the above, by Hooke's law,

$$\mathbf{\ddot{u} = \quad * \Delta} \tag{12}$$

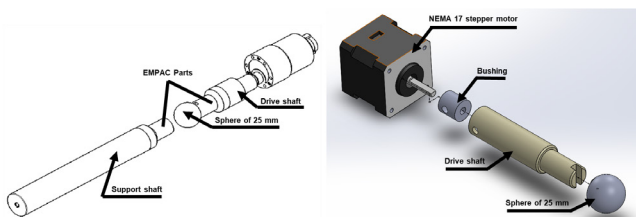From the above, the value of the constant K of the spring is cleared.

$$\mathbf{K = \dfrac{F}{\Delta x}} \tag{13}$$

Replacing the values of the sphere force and the distance differential Δx expressed in meters yields:

$$\mathbf{K = \dfrac{1{,}19\,Newton}{0{,}014\,m}} \tag{14}$$

$$\mathbf{K = 85{,}35\,\dfrac{N}{m}} \tag{15}$$

The spring constant K to be used in the plunger system to hold the sphere must be $K = 85{,}35\,\frac{N}{m}$

Figure 11. Motor system, drive shaft, and bushing: a) current b) redesigned
Source: Authors

The implementation of the stepper motor (Figure 11) was the most representative change made to the system, which allows controlling the position of the sphere, its velocity, and the direction of its rotation. In this case, the system was tested while considering hip joint replacements as reference.

The Nema 17 stepper motor was configured to travel 1,8° per step, which allows for a relation to be established, so that the sphere can travel at a certain angle. The rotation velocity of the motor is varied by pulse width modulation (PWM), which makes the motor versatile for the proposed implementation.

Results (testing)

Testing was performed with equipment that allows assessing wear. This equipment has a base where there is a lever arm with counterweights, which, from their distance to the center, apply a certain load to the sample under analysis. To determine the load exerted by the dead weight and the counterweight, a dynamometer is used. Moreover, there is a sphere, which rotates against the sample for a number of cycles and at a certain velocity, producing wear and abrasion on the sample.

The sphere is coupled between two coaxial shafts, one of which is supported on a bearing and coupled to a bipolar DC stepper motor, which ensures the velocities and angles of rotation of the sphere during the tests, while the other one has a plunger system to exert a force between the sphere and the other shaft in order to keep the sphere in a single position. There is a control module in charge of the whole system, from which parameters such as the test time, the angle of rotation, and the velocity of the sphere during the test can be varied (Figure 12).

We initially planned to carry out dry tests, with the aim to observe the general behavior of the system and analyze the traces left on the samples subjected to the test.
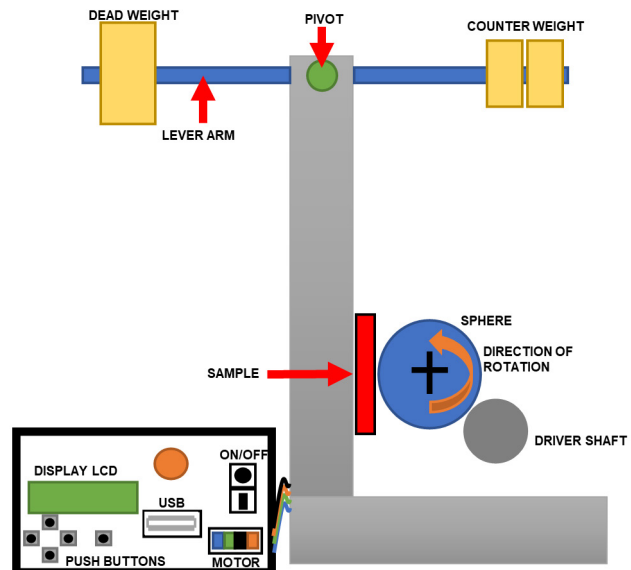
Figure 12. General scheme of the micro-abrasion tests
Source: Authors

It is also important to highlight the use of suitable materials in joint replacements, specifically those used in hip prostheses, where biocompatible steels are used for the femoral head, as well as ultra-high molecular weight polyethylene (UHMWPE) for the acetabular cup (Figure 13) (Diomidis *et al.*, 2012).
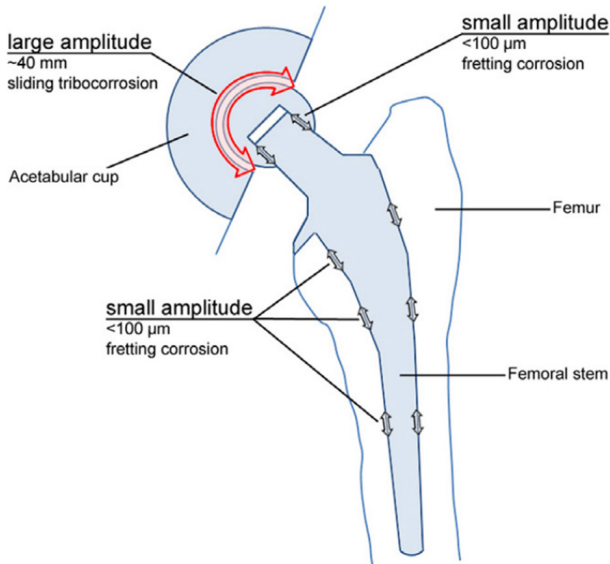
Figure 13. Hip replacement diagram
Source: Diomidis *et al.* (2012)

The samples used in the tests were previously polished until a low surface roughness was obtained. This was done using silicon carbide (SiC) abrasive paper, increasing the size from 100 to 1 200 and finally polishing the specimens with a 0,05-micron alumina (Al2O3) suspension on a rotating disk. Once the samples were polished, they were cleaned with ultrasound equipment, immersing them completely in ketone. Then, the samples were dried, and assembly was carried out in the system. The parameters of the test were adjusted as mentioned below:

- ✓ The applied load was adjusted by moving the dead weight and the counterweight while measuring the force with a dynamometer. For this case, a constant load of 2 N was set by securing the masses with nuts.
- ✓ The sphere was positioned on the drive shaft, and it was later adjusted by moving the support shaft.
- ✓ The specimen was clamped to the system with the help of a 3D-printed clamping piece.
- ✓ The lever arm was lowered so that the specimen gently touched the sphere.
- ✓ The user control module was used to set the time of the test, the speed of the sphere, and a normal or a reciprocating rotation.
- ✓ Finally, the equipment was started and, when the test was complete, the specimen was carefully removed.

At the end of the test, the sphere and the sample were cleaned again, and the wear tracks were analyzed by means of scanning electron microscopy (SEM).

For the tests, two sphere rotation speeds were determined, one of these being the normal walking speed of a person, which is about 1 Hz. Each leg makes 1 cycle in 1 second, so, in 1 minute, there are 60 cycles, which means that the sphere must rotate at a speed of 60 Rev/min to recreate this frequency. The second speed was estimated to be twice the first one (120 Rev/min) (Lavernia and Alcerro, 2008; OrthoInfo, n.d.).

For joint replacements, there is a normal load of approximately 70 or 80 Newtons that falls between the femoral area and the tibial or acetabular component (Cañizo *et al.*, 2010). In all tests, a constant load of 2 Newtons was applied to maintain this parameter controlled, while varying other parameters such as the angles of travel of the sphere and the velocity. These values were chosen to closely resemble those observed in a real environment.

In one-way and reciprocating rotation testing, a test time of 30 minutes, a sample material of L 316 steel, and a sphere material of AISI 52100 steel in contact with the sample are used (Gee *et al.*, 2002).

During testing with different angles of travel, it has been found that the hip can reach a flexion angle of 113° and an extension angle of 28°, which means that one of the angles to be examined is 113. The other angle is the sum of the flexion and extension angles, which is 141° (Boone and Azen, 1979). In hip joint replacements, one must consider the pressure that exists on the articular surface, which is transmitted by the acetabulum towards the femoral head, which means that the forces present in the hip act on a spherical area that is delimited by two planes at 76° (Figure 14) (Cañizo *et al.*, 2010). Thus, 76° should also be included in the tests. Finally, the intermediate angles should also be evaluated, *i.e.*, 45 and 90°.
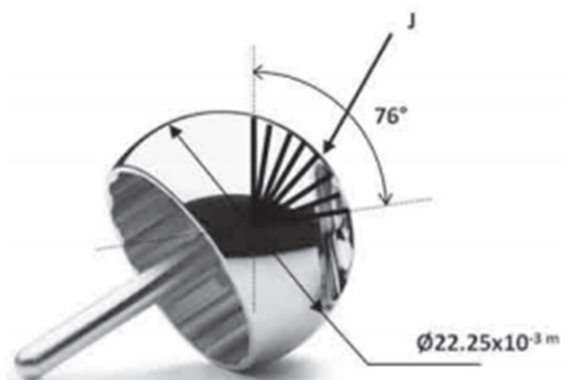
Figure 14. Load acting on the spherical bone
Source: Cañizo *et al.* (2010)

Table 2 shows the testing parameters.

Within each test, two tests are performed, from which two wear constants are obtained and averaged in order to obtain a wear constant for each case evaluated.

Table 2. Wear test specifications

Sample material	Steel L 316
Sphere material	Steel AISI 52100
Normal load	2 Newtons
Velocity 1	60 RPM
Velocity 2	120 RPM
Continuous rotation	360˚
Angle 1	76˚
Angle 2	141˚
Angle 3	113˚
Angle 4	45˚
Angle 5	90˚
Test time	30 minutes

Source: Authors

Results and discussion

Stereoscopy and SEM analysis

Figure 15 shows one of the images of the wear grooves taken by a stereoscope, where the lines generated by the micro-abrasive wear mechanism for dry testing can be seen. In addition, it was observed that, once the test is finished, the specimen shows material adherence by the sphere, which is why, before analyzing them by means of SEM, the sample was cleaned with ultrasound equipment in order to appreciate the morphology of the sample.


Figure 15. Track dry wear test with stereoscope
Source: Authors

Once the samples had been examined with the stereoscope, the morphology of the sample was examined via SEM, as shown in Figure 16.

In Figures 16a and 16b, the borders of the craters generated by the tests exhibit a regular circular limit, which characterizes a centered movement of the sphere during testing (Uehara et al., 2019). Additionally, it can be seen that there is wear in the studied cases, which is generally classified as slight

or severe. The distinction is based on the marks left or produced by the wear. Slight wear follows a uniform pattern of defined and shallow lines, while severe wear shows a greater depth in the wear tracks, and amorphous zones may appear (Pérez-Oviedo and Torre-Nieto, 2015).

Figure 17 details a footprint with patterns that meet the description of slight wear. The wear reported by the samples analyzed in all cases is slight, without the presence of abrasive wear, where grooves are generally denoted along the entire length of the crater, with possible drilling points (Cozza, 2013).
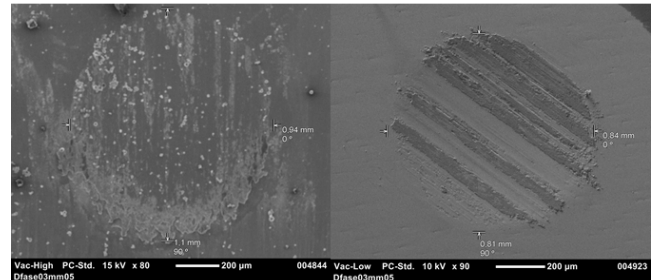
Figure 16. Wear test traces: (a) single direction of rotation at 60 RPM, dry; (b) reciprocating rotation at 120 RPM and 90˚, dry
Source: Authors
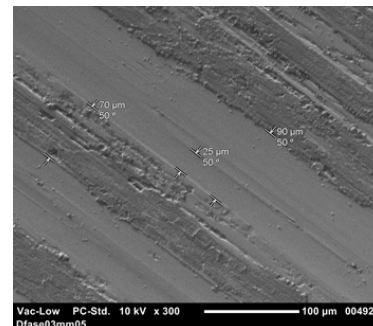
Figure 17. Track dry wear test with reciprocating rotation at 120 RPM and at 90˚
Source: Authors

Wear rate estimation

The measurements carried out in each track correspond to the diameter, measured both vertically and horizontally. The values obtained are then averaged. Afterwards, the wear volume of each test (Equation (1)) is calculated while considering the radius of the sphere, which is $R_{sphere} = 0,0125m$.

Finally, the wear coefficient for each test must be calculated (Equation (3)), where the total sliding distance of each test and the average of the previously measured track must be used.

By performing two tests for each experiment, two wear coefficients are obtained, which are averaged to obtain a single value. Table 3 shows the wear constants K_c for the tests performed. The units of the wear coefficient are $K_c = \left[\frac{m^2}{N} \right]$.
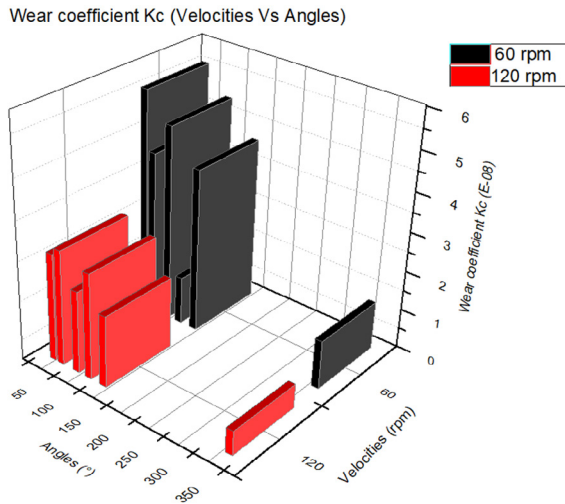
Table 3. Wear coefficient K_c as a function of the velocities and the angles traveled by the sphere during testing

	Velocities	
Angles (Grades)	60 RPM (1x10⁻⁸)	120 RPM (1x10⁻⁸)
45	5,58	2,7
76	4,12	2,91
90	4,94	2,07
113	1,19	2,67
141	4,13	1,81
Continuous rotation (360)	1,23	0,62

Source: Authors

From the data in Table 3, a graph is made with the data shown.

Figure 18. Graph of the wear coefficient Kc (velocities *vs.* angles)
Source: Authors

In Figure 18, a trend is observed among the tests; in five of the six cases, there is a higher wear coefficient at low revolutions (60 RPM).

Conclusions

With the upgrade made to the equipment's subsystems for wear and micro-abrasion tests, the system became variable and open to changes; with the implementation of the reciprocating travel angles, different tests can be performed which allow for a mor realistic observation of the behavior of biomaterials, resembling the travel angles of a certain joint, which opens the possibility of studying these biomaterials from more specific approaches.

The modifications to the equipment made it possible to carry out wear testing with variations in the different angles of travel and with the inversion of rotation, obtaining more defined tracks and allowing for an easy analysis. This, in comparison with the tracks obtained before the upgrade.

As for the tests performed, it is evident that, in most cases, there was an adherence of the sphere material (AISI 52100 steel) to the sample, which implies a slight wear.

Finally, with the tests performed, there is a tendency indicating that, as the contact angle of the sphere decreases for reciprocating tests, the wear coefficient increases.

References

Ardila, M. A. N., Costa, H. L., and de Mello, J. D. B. (2020). Influence of the ball material on friction and wear in microabrasion tests. *Wear*, *450-451*, 203266. https://doi.org/10.1016/j.wear.2020.203266

BBC (n.d.). BBC Mundo — Noticias — Somos 7.000 millones, ¿cuáles son los desafíos? *BBC News*. https://www.bbc.com/mundo/noticias/2011/10/111026_poblacion_informe_am

BBC (2012). ¿Cuántos habitantes tendrá el planeta en 2050? ¿Y en 2300? *BBC News*. https://www.bbc.com/mundo/noticias/2012/10/121014_poblacion_futuro_habitantes_dp

Boone, D. C., and Azen, S. P. (1979). Normal range of motion of joints in male subjects. *The Journal of Bone and Joint Surgery, American Volume*, *61*(5), 756-759. https://doi.org/10.2106/00004623-197961050-00017

Caballero, J. L., Sierra Melo, N., and Aperador Chaparro, W. (2016). Design and construction of a machine for micro-abrasion-corrosion testing in simulated biological environments. *Tecciencia*, *11*(20), 5-18. https://doi.org/10.18180/tecciencia.2016.20.2

Caicedo, J. C., Aperador, W., and Aguilar, Y. (2013). Tribological performance evidence on ternary and quaternary nitride coatings applied for industrial steel. *Revista Mexicana de Física*, *59*(4), 364-373.

Cañizo, R. G. R., García, L. A. G., Torres, M. V., Cruz, E. A. M., and Pineda, J. M. S. (2010). Análisis experimental del desgaste entre UHMWPE y acero inoxidable 316l empleados en la manufactura de prótesis coxofemorales. *Revista Colombiana de Biotecnología*, *12*(2), 2.

Cozza, R. C. (2013). A study on friction coefficient and wear coefficient of coated systems submitted to micro-scale abrasion tests. *Surface and Coatings Technology*, *215*, 224-233. https://doi.org/10.1016/j.surfcoat.2012.06.088

Cozza, R. C., Tanaka, D. K., and Souza, R. M. (2009). Friction coefficient and abrasive wear modes in ball-cratering tests conducted at constant normal force and constant pressure – Preliminary results. *Wear*, *267*(1), 61-70. https://doi.org/10.1016/j.wear.2009.01.055

Dieter, G., and Schmidt, L. (2009). *Engineering design*. McGraw-Hill Education.

Diomidis, N., Mischler, S., More, N. S., and Roy, M. (2012). Tribo-electrochemical characterization of metallic biomaterials for total joint replacement. *Acta Biomaterialia*, *8*(2), 852-859. https://doi.org/10.1016/j.actbio.2011.09.034

Gant, A. J., and Gee, M. G. (2011). A review of micro-scale abrasion testing. *Journal of Physics D: Applied Physics*, *44*(7), 073001. https://doi.org/10.1088/0022-3727/44/7/073001

Gee, M. G., Gant, A., Hutchings, I., Bethke, R., Schiffmann, K., Acker, K. V., Poulat, S., and Gachon, Y. (2002). *Ball cratering or micro-abrasion wear testing of coatings*. National Physical Laboratory. https://eprintspublications.npl.co.uk/2545/1/mgpg57.pdf

Gómez, M., and Sabeh, N. E. (n.d.). *Calidad de vida: evolución del concepto y su influencia en la investigación y la práctica*. http://campus.usal.es/~inico/investigacion/invesinico/calidad.htm

Lavernia, D. C. J., and Alcerro, D. J. C. (2008). Artroplastia total de rodilla. *Actualidades de Posgrado para el Médico General, 13*(7), 6-11.

Losada-Prieto, C., Om-tapanes, N., and Rodríguez, J. (2001). Tribología y lubricación en ensayo de banco. *CIENCIA Ergo-Sum, 8*(2), 184-190.

OrthoInfo (n.d.) *Reemplazo total de rodilla*. https://www.orthoinfo.org/es/treatment/reemplazo-total-de-rodilla-total-knee-replacement/

Pérez-Oviedo, P., and Torre-Nieto, J. (2015). Guía de diseño para calcular el desgaste abrasivo entre componentes no lubricados. *Ciencia, Ingeniería y Desarrollo Tec Lerdo, 1*(1), 20-29. http://revistacid.itslerdo.edu.mx/coninci2015/Revista%20CID%20Tec%202015.pdf

Rasor, J. S. (2009, March 29). The science of friction. *Verdict Medical Devices*. https://www.medicaldevice-network.com/features/feature52481/

Sampaio, M., Buciumeanu, M., Henriques, B., Silva, F. S., Souza, J. C. M., and Gomes, J. R. (2016). Comparison between PEEK and Ti6Al4V concerning micro-scale abrasion wear on dental applications. *Journal of the Mechanical Behavior of Biomedical Materials, 60*, 212-219. https://doi.org/10.1016/j.jmbbm.2015.12.038

Stachowiak, G. B., Stachowiak, G. W., and Brandt, J. M. (2006). Ball-cratering abrasion tests with large abrasive particles. *Tribology International, 39*(1), 1-11. https://doi.org/10.1016/j.triboint.2004.10.010

Staia, M. H., Enriquez, c. E., Puchi, E. S., Lewis, D. B., and Jeandin, M. (1998). Application of ball cratering method to study abrasive wear. *Surface Engineering, 14*(1), 49-54. https://doi.org/10.1179/sur.1998.14.1.49

Uehara, P. N., Iegami, C. M., Tamaki, R., Ballester, R. Y., de Souza, R. M., and Laganá, D. C. (2019). Analysis of behavior of the wear coefficient in different layers of acrylic resin teeth. *The Journal of Prosthetic Dentistry, 121*(6), P967.E1-967.E6. https://doi.org/10.1016/j.prosdent.2019.02.022

Vallet, R. M. (2004). *Biomateriales para sustitución y reparación de tejidos*. https://www.aecientificos.es/biomateriales-para-sustitucion-y-reparacion-de-tejidos/